Determining the long living quasi-normal modes of relativistic stars*

Lü Jun-Li(吕君丽)[a)†] and Suen Wai-Mo(孙纬武)[b)c)]

[a)] College of Physics and Information Science, Hunan Normal University, Changsha 410081, China

[b)] Department of Physics, Washington University, One Brookings Drive, St. Louis, MO 63130, USA

[c)] Department of Physics, Chinese University of Hong Kong, Shatin, Hong Kong, China

(Received 13 September 2010; revised manuscript received 6 November 2010)

Methods of finding quasi-normal modes of non-rotating relativistic stars have been well established, however, none of the existing treatments which take spacetime and fluid oscillations fully into account can determine modes of long decay time, e.g., the p and g mode series, or the f modes for stars with low compactness ratio (M/R). In this paper we show how the quasi-normal modes of long lifetime can be determined through refinements of a treatment originally due to Detweiler and Lindblom. The determination of the p mode series has been argued in the literature to have implication on the life time of gravitational wave sources and stellar stability. In this paper we 1) provide detailed steps in our treatment to facilitate future effort in this direction; 2) correct mistakes in the literature on the formulation; and 3) analyse the accuracy of the quasi-normal mode frequencies obtained and the limitations of the treatment.

Keywords: relativistic stars, non-radial perturbations, gravitational wave, quasi-normal modes

PACS: 04.20.–q, 04.25.D–, 04.30.–w **DOI:** 10.1088/1674-1056/20/4/040401

1. Introduction

The detection and the associated theoretical and numerical studies of gravitational radiations have attracted much attention in the last ten years, with gravitational wave observatories coming online and being built.[1−3] This paper focuses on the calculation of gravitational radiations from stellar oscillations. Significant efforts in this direction include Refs. [4]–[51].

The main aim of this paper is to enable the accurate determination of the quasi-normal mode (QNM) frequency of relativistic stars and in particular those frequencies having an imaginary part $\omega_{\rm I}$ many orders of magnitudes smaller than the real part $\omega_{\rm R}$. It is well known that for relativistic stars with relatively large compactness ratio, i.e., M/R of order 10^{-1}, the highly damped QNMs, including axial modes and the various branches of W modes that are predominantly spacetime oscillations, have comparable real and imaginary parts, i.e., $Q = \omega_{\rm R}/(2\omega_{\rm I})$ of order 1. On the other hand, the polar modes that are strongly tied to fluid oscillations are slowly damped. Among them the fundamental mode (f mode) typically has Q of order 10^4 for most equations of state (EOSs), see, e.g., Ref. [26]. The lowest p mode has Q of order 10^5,[26] and the higher p modes would have a Q one or more orders of magnitude larger. The g modes has Q of order 10^8 or larger. The large Q values indicate the existence of two very different scales in the problem, and that presents a difficulty for the accurate numerical determination of the complex QNM frequency. While the g modes may not play an important role in the near future in asteroseismology due to the difficulty in their detection[40−44] (however, they might be relevant to gravitational radiations from proto neutron stars, see Refs. [43], [52], and [53] and citations therein), the p modes may be of significance in gravitational wave observations. It has been argued in Ref. [24], which managed to push the determination of QNMs to $Q \sim 10^6$, that the lowest few p modes exhibit unexpected behaviour and that a study of the p modes may have implications for questions regarding stellar stability and the lifetime of gravitational wave sources.

The above facts are for the case of stars with large compactness ratio, $M/R \sim 10^{-1}$. For less compact stars with $M/R \sim 10^{-2}$ or smaller, even the f mode would have a Q of order 10^6 or 10^7 and cannot be accurately determined by existing treatments that we

*Project supported by the Science Foundation of the Education Department of Hunan Province of China (Grant No. 07c578) and in part by the US National Science Foundation NRAC, the McDonnell Center for the Space Sciences of the Washington University (Grant No. MCA93S025).

†Corresponding author. E-mail: lujunli61@163.com

© 2011 Chinese Physical Society and IOP Publishing Ltd

are aware of. In this paper we push for an accurate determination of both the real and imaginary parts of the QNM frequencies for large values of Q, i.e., the long living QNMs, in a treatment based on the formulation of Detweiler and Lindblom[9,10] for non-rotating stars. We note that a large Q may mean that other damping mechanisms, e.g., neutrino radiation or fluid viscosity, are more significant than the damping due to gravitational radiations. However, the determination of the imaginary part of the frequency of such QNMs would still be of interest as it gives the gravitational radiation power of the modes.

There are two main approaches in the calculation of stellar QNMs that treat the coupled spacetime and fluid oscillations in full without simplifying assumptions for non-rotating stars. The first approach was pioneered by Thorne and collaborators.[4−8] Thorne *et al.* developed a fifth-order system of ordinary differential equations that described the non-radial perturbations of relativistic stellar models. The formulation in a natural way extended the Newtonian treatment[54] to fully relativistic stars. However, the system has singular behaviour both at the centre and the surface of the star that makes its numerical implementation difficult. Detweiler and Lindblom simplified the system of Ref. [4] to a fourth-order set[9,10] with less singular properties, and applied it to obtain the QNMs of various relativistic stellar models.[13] As indicated in Ref. [26], the treatment in Ref. [13] is good up to $Q \sim 10^5$. The treatment of Ref. [26] made use of the formulation of Detweiler and Lindblom,[9,10] but with the radial coordinate r extended to the complex plane in the region exterior to the star. The first few p modes with $Q \sim 10^6$ have been calculated with the imaginary part determined to single digit of precision. Our paper pushes further in this direction.

In the second approach developed by Chandrasekhar and Ferrari,[11,12] relativistic stellar oscillation is treated as an extension of the perturbation theory of the Schwarzschild black holes, instead of an extension of the Newtonian treatment. The treatment yields a fifth-order system (it can also be reduced to fourth-order but with a more complicated set of equations[18]) based only on the spacetime variables. The system has singular behaviour only at the centre of the star and is significantly simpler for the calculations of the QNMs. It is capable of determining accurately the frequencies of the modes which are describing predominantly the oscillations of the spacetime, like the axial modes and the w modes, which are highly damped. For our aim of calculating slowly damped modes, which are predominantly fluid oscillation modes, and modes for stars with low compactness ratio (closer to the Newtonian limit), the first approach seems to be more promising. We note that there are also other promising approaches, e.g., Ref. [39], the properties of which are not fully explored in the literature.

In this paper we push the determination of QNM frequencies to at least $Q \sim 10^8$ with imaginary parts having 3 digits of precision. This would enable the determination of a good part of the p mode spectrum for a reasonably large set of EOSs and a range of stellar models with compactness ratio M/R less than 10^{-1}. Other points to note of this paper are: 1) we provide detailed steps and intermediate results of our treatment, as well as the ways to choose the numerical parameters, to facilitate future effort in this direction in calculating in particular QNMs with high Q factors; 2) we correct for mistakes in the formulation[9,10] on which our treatment is based; and 3) we provide an analysis for the accuracy of the QNM frequencies obtained, a step that is important for any numerical treatment but often missing.

The arrangement of the paper is as follows. In Section 2, we give for completeness the full set of perturbation equations[9,10] of the non-radial pulsations of relativistic stars, and the boundary conditions at the centre ($r = 0$) and the surface of the star ($r = R$). This set of differential equations has singularity at $r = 0$. At $r = R$, the physical boundary conditions to be imposed (i.e. the Lagrangian perturbation of pressure goes to zero) leads to another singularity that also affects the accuracy of numerical implementations. We find a missing factor of 2 in one equation of Ref. [9] (henceforth LD) that has a small effect on the QNM frequencies for the stellar models we checked.

In Section 3, we describe in detail our numerical implementation of the DL/LD formulation. Using the case of a polytropic EOS, we give explicit results at crucial steps of our numerical implementation, discuss how various numerical parameters are to be chosen, and how the choices affect the final results. Through a careful choice of the numerical parameters as discussed in this section, we can obtain frequencies with Q up to 10^8 but with precisions less than desired.

In Section 4, we study the accuracy of the QNM frequencies obtained. There are three types of error in our treatment: (i) errors associated with computer precision, (ii) finite differencing error in numerical integration and error of linear solver algorithm, and (iii) errors introduced by the approximations used in the treatment, namely, (a) the approximation associated

with the singularity at the centre of the star, (b) the approximation associated with the singularity at the boundary of the star and (c) the approximation used at infinity (outer boundary of the computational grid) for the determination of the complex QNM frequency using a set of real frequencies.

Error sources (i) and (ii) are no concern, with the speed and memory size of modern computers and modern numerical algorithms; one can use quadruple or higher precision if necessary. For numerical integration, a predictor–corrector algorithm as used in our implementation guarantees the overall error of integration to be smaller than a prescribed value. Typically we take it to be 10^{-12}, which is enough in view of the error type (iii). Of more concern are the errors (iii(a)–iii(c)). We provide in Section 3 detailed analyses of (iii(a)) and (iii(b)), including the dependence of the resulting QNM frequencies on the numerical choices used in the approximations. An analysis of (iii(c)), the error associated with the expansion of the outgoing wave amplitude $A(\omega)$, is more complicated. In Setion 3 we will see that if one goes into using higher order terms in the expansion, more points of the real frequency inputs would have to be used. The best range of the real frequencies used as inputs cannot be determined a priori, which depends on the magnitude of the imaginary part of the frequency to be determined. Instead of going into a detailed study of this error source, we carry out an additional step to determine the overall accuracy of the QNM frequency ω obtained: For each complex frequency ω found, we can construct the corresponding set of complex eigenfunctions that satisfy the boundary conditions at the centre and at the surface of the star. At the outer boundary of the computational domain, provided that it is at a large enough radius, the eigenfunctions represent an outgoing wave with amplitude $A(\omega)$ and an incoming wave with amplitude $B(\omega)$. One can then evaluate the accuracy of ω as a QNM frequency by the ratio $S(\omega) = |B(\omega)/A(\omega)|$ where $|\quad|$ denotes taking absolute value. The error associated with the finiteness of the computational domain can be determined through a convergence test of increasing the computational domain size.

This additional step also provides a mean to improve the accuracy of the QNM frequency found. It is well known that the QNMs are sharp resonances; $S(\omega)$ is an extremely sensitive function of ω. For an accurate enough initial trial ω, i.e., an ω obtained through the treatment given in Section 3, one can do a two-dimensional (2D) search for the real and imaginary parts of ω that minimize $S(\omega)$. It is through this we obtain QNM frequencies with $Q \sim 10^8$ and with imaginary parts having 3 digits of precision. In principle there is no obstacle to further improving the result with more computational resources.

The last section contains a brief conclusion.

2. The perturbation equations and the boundary conditions

For completeness we give the complete set of equations in this section. They are contained in LD[9] and DL[10] up to the minor corrections mentioned above.

2.1. The unperturbed system

The general static spherically symmetric metric which describes the geometry of a static star can be written as

$$\mathrm{d}s^2 = -\mathrm{e}^{2\nu}\mathrm{d}t^2 + \mathrm{e}^{2\lambda}\mathrm{d}r^2 + r^2(\mathrm{d}\theta^2 + \sin^2\theta\mathrm{d}\phi^2). \quad (1)$$

Here ν and λ are functions of the radial coordinate r. The Tolman–Oppenheimer–Volkov (TOV) equations for the metric are

$$\frac{\mathrm{d}M}{\mathrm{d}r} = 4\pi r^2\rho, \quad (2)$$

$$\frac{\mathrm{d}p}{\mathrm{d}r} = -\frac{(\rho+p)(M+4\pi r^3 p)}{r(r-2M)}, \quad (3)$$

$$\frac{\mathrm{d}\nu}{\mathrm{d}r} = -\frac{1}{(\rho+p)}\frac{\mathrm{d}p}{\mathrm{d}r}, \quad (4)$$

where $M(r)$ is defined as

$$M(r) = \frac{1}{2}r(1-\mathrm{e}^{-2\lambda}), \quad (5)$$

which represents the gravitational mass inside the radius r. Here ρ is the total energy density, p is the pressure, both are measured in the proper frame of the fluid.

The boundary conditions that lead to an equilibrium stellar model are given by: i) At $r = 0$, the absence of a singularity implies $\lambda(r = 0) = 0$ and $M(r = 0) = 0$. ii) At the surface of the star R, the pressure goes to zero and $2\nu(r = R) = \ln(1 - 2M(r = R)/R)$. With these conditions a value of the central density ρ_0 (less than a certain critical value) leads to a unique solution of the TOV equations for a given EOS $p = p(\rho)$.

2.2. The perturbed system

With the functions of perturbation of DL,[10] the perturbed metric can be written as

$$\begin{aligned} \mathrm{d}s^2 = & -\mathrm{e}^{2\nu}(1+r^l H_0 Y_m^l \mathrm{e}^{\mathrm{i}\,\omega t})\mathrm{d}t^2 \\ & -2\,\mathrm{i}\,\omega r^{l+1} H_1 Y_m^l \mathrm{e}^{\mathrm{i}\,\omega t}\mathrm{d}t\mathrm{d}r \\ & +\mathrm{e}^{2\lambda}(1-r^l H_0 Y_m^l \mathrm{e}^{\mathrm{i}\,\omega t})\mathrm{d}r^2 \\ & +r^2(1-r^l K Y_m^l \mathrm{e}^{\mathrm{i}\,\omega t})(\mathrm{d}\theta^2+\sin^2\theta\mathrm{d}\phi^2). \end{aligned} \tag{6}$$

The perturbation of the fluid in the star is described by the Lagrangian displacement vector ξ^α in terms of the perturbation functions $W(r)$ and $V(r)$

$$\xi^r = r^{l-1}\mathrm{e}^{-\lambda} W(r) Y_m^l \mathrm{e}^{\mathrm{i}\,\omega t}, \tag{7a}$$

$$\xi^\theta = -r^{l-2} V(r) \partial_\theta Y_m^l \mathrm{e}^{\mathrm{i}\,\omega t}, \tag{7b}$$

$$\xi^\phi = -r^l (r\sin\theta)^{-2} V(r) \partial_\phi Y_m^l \mathrm{e}^{\mathrm{i}\,\omega t}. \tag{7c}$$

Four of the five perturbation functions H_0, H_1, K, V, and W are independent. Their relations are given by

$$\begin{aligned} & \left[3M+\frac{1}{2}(l+2)(l-1)r+4\pi r^3 p\right]H_0 \\ & = 8\pi r^3 \mathrm{e}^{-\nu} X - \left[\frac{1}{2}l(l+1)(M+4\pi r^3 p)-\omega^2 r^3 \mathrm{e}^{-2(\lambda+\nu)}\right]H_1 \\ & \quad + \left[\frac{1}{2}(l+2)(l-1)r-\omega^2 r^3 \mathrm{e}^{-2\nu}-r^{-1}\mathrm{e}^{2\lambda}(M+4\pi r^3 p)(3M-r+4\pi r^3 p)\right]K. \end{aligned} \tag{8}$$

LD/DL[9,10] introduced a new function $X(r)$ to replace $V(r)$. The equations of perturbation in terms of $X(r)$ are

$$K_{,r} = r^{-1}H_0 + \frac{1}{2}l(l+1)r^{-1}H_1 - \left[(l+1)r^{-1}-\nu_{,r}\right]K - 8\pi(\rho+p)\mathrm{e}^{\lambda}r^{-1}W, \tag{9a}$$

$$H_{1,r} = -r^{-1}\left[l+1+2M\mathrm{e}^{2\lambda}r^{-1}+4\pi r^2\mathrm{e}^{2\lambda}(p-\rho)\right]H_1 + r^{-1}\mathrm{e}^{2\lambda}\left[H_0+K-16\pi(\rho+p)V\right], \tag{9b}$$

$$W_{,r} = -(l+1)r^{-1}W + r\mathrm{e}^{\lambda}\left[(\gamma p)^{-1}\mathrm{e}^{-\nu}X - l(l+1)r^{-2}V + \frac{1}{2}H_0 + K\right], \tag{9c}$$

$$\begin{aligned} X_{,r} = & -lr^{-1}X + (\rho+p)\mathrm{e}^{\nu}\left\{\frac{1}{2}(r^{-1}-\nu_{,r})H_0 + \frac{1}{2}\left[r\omega^2\mathrm{e}^{-2\nu}+\frac{1}{2}l(l+1)r^{-1}\right]H_1 + \frac{1}{2}(3\nu_{,r}-r^{-1})K\right. \\ & \left. - l(l+1)\nu_{,r}r^{-2}V - r^{-1}\left[4\pi(\rho+p)\mathrm{e}^{\lambda}+\omega^2\mathrm{e}^{\lambda-2\nu}-r^2(r^{-2}\mathrm{e}^{-\lambda}\nu_{,r})_{,r}\right]W\right\}. \end{aligned} \tag{9d}$$

Here γ is the adiabatic index and comma r denotes a derivative with respect to r. The perturbation function $X(r)$ is related to W and V by

$$\begin{aligned} X = & \omega^2(\rho+p)\mathrm{e}^{-\nu}V - r^{-1}p_{,r}\mathrm{e}^{(\nu-\lambda)}W \\ & + \frac{1}{2}(\rho+p)\mathrm{e}^{\nu}H_0. \end{aligned} \tag{10}$$

Equation (10) is equation (6) in Ref. [10], up to a correction of a typo (the first term of equation (6) in the paper has a factor of ω^3).

This system of equations forms a fourth-order system of linear differential equations. For each choice of suitable l and ω, there exist four linearly independent solutions. The physical solution must satisfy the appropriate boundary conditions, i.e., (i) the perturbation functions must be finite everywhere, especially at the centre of the star where the system becomes singular for $r=0$; (ii) the perturbed pressure must vanish at the surface of the star $r=R$, under the present choice of gauge condition. This implies that the function X must vanish at $r=R$. There is only one solution which satisfies all of the boundary conditions for a given set of l and ω.

As the system is singular at $r=0$, we expand the perturbation functions in power of r at $r=0$. It is easy to see that the expansion has no odd power terms, i.e., denoting $Y(r)=\{H_1, K, W, X\}$,

$$Y(r) = Y(0) + \frac{1}{2}Y_{,rr}(0)r^2 + O(r^4). \tag{11}$$

The coefficients $Y(0)$ and $Y_{,rr}(0)$ are determined by substituting Eqs. (11) into Eqs. (9). The lowest order coefficient $Y(0)$ satisfies the relations

$$H_0(0) = K(0), \tag{12}$$

$$H_1(0) = \frac{1}{l(l+1)}\left[2lK(0)+16\pi(\rho_0+p_0)W(0)\right], \tag{13}$$

$$\begin{aligned} X(0) = & (\rho_0+p_0)\mathrm{e}^{\nu_0}\left\{\left[\frac{4\pi}{3}(\rho_0+3p_0)-\omega^2\mathrm{e}^{-2\nu_0}l^{-1}\right]\right. \\ & \left.\times W(0)+\frac{1}{2}K(0)\right\}. \end{aligned} \tag{14}$$

This implies that there are two constants freely specifiable at $r = 0$. The second-order terms $Y_{,rr}(0)$ satisfy the relations

$$\begin{aligned}
&-\frac{1}{4}(\rho_0+p_0)K_{,rr}(0)+\frac{1}{2}\left[p_2+\omega^2(\rho_0+p_0)\frac{(l+3)}{l(l+1)}\mathrm{e}^{-2\nu_0}\right]W_{,rr}(0)+\frac{1}{2}\mathrm{e}^{-\nu_0}X_{,rr}(0)\\
=&\frac{1}{2}\nu_2\mathrm{e}^{-\nu_0}X(0)+\frac{1}{4}(\rho_2+p_2)K(0)+\frac{1}{4}(\rho_0+p_0)Q_0+\frac{1}{2}\omega^2(\rho_0+p_0)\mathrm{e}^{-2\nu_0}Q_1\\
&-\left\{p_4-\frac{4\pi}{3}\rho_0p_2+\frac{\omega^2}{2l}\left[\rho_2+p_2-2(\rho_0+p_0)\nu_2\right]\mathrm{e}^{-2\nu_0}\right\}W(0), \qquad (15a)\\
&-\frac{1}{4}l(l+1)H_{1,rr}(0)+\frac{1}{2}(l+2)K_{,rr}(0)+4\pi(\rho_0+p_0)W_{,rr}\\
=&\frac{4\pi}{3}(\rho_0+3p_0)K(0)+\frac{1}{2}Q_0-4\pi\left[\rho_2+p_2+\frac{8\pi}{3}\rho_0(\rho_0+p_0)\right]W(0), \qquad (15b)\\
&-\frac{1}{8}l(l+1)(\rho_0+p_0)\mathrm{e}^{\nu_0}H_{1,rr}(0)+\frac{1}{2}(l+2)X_{,rr}(0)\\
&-\frac{1}{2}(\rho_0+p_0)\mathrm{e}^{\nu_0}\left[(l+2)\nu_2-4\pi(\rho_0+p_0)-\omega^2\mathrm{e}^{-2\nu_0}\right]W_{,rr}\\
=&\frac{1}{2}\left[\rho_2+p_2+(\rho_0+p_0)\nu_2\right]\frac{l}{(\rho_0+p_0)}X(0)+(\rho_0+p_0)\mathrm{e}^{\nu_0}\left\{\nu_2K(0)\right.\\
&+\frac{1}{4}Q_0+\frac{1}{2}\omega^2\mathrm{e}^{-2\nu_0}H_1(0)-\frac{1}{2}l(l+1)\nu_2Q_1+\left[(l+1)\nu_4-2\pi(\rho_2+p_2)\right.\\
&\left.\left.-\frac{16\pi^2}{3}\rho_0(\rho_0+p_0)+\left(\nu_4-\frac{4\pi}{3}\rho_0\nu_2\right)+\omega^2\mathrm{e}^{-2\nu_0}\left(\nu_2-\frac{4\pi}{3}\rho_0\right)\right]W(0)\right\}, \qquad (15c)\\
&\frac{1}{2}(l+3)H_{1,rr}(0)-K_{,rr}(0)-8\pi(\rho_0+p_0)\frac{l+3}{l(l+1)}W_{,rr}\\
=&4\pi\left[\frac{1}{3}(2l+3)\rho_0-p_0\right]H_1(0)+\frac{8\pi}{l}(\rho_2+p_2)W(0)-8\pi(\rho_0+p_0)Q_1+\frac{1}{2}Q_0, \qquad (15d)
\end{aligned}$$

where Q_0 and Q_1 are defined by

$$\begin{aligned}
Q_0 =& \frac{4}{(l+2)(l-1)}\left\{8\pi\mathrm{e}^{-\nu_0}X(0)-\left(\frac{8\pi}{3}\rho_0+\omega^2\mathrm{e}^{-2\nu_0}\right)K(0)\right.\\
&\left.-\left[\frac{2\pi}{3}l(l+1)(\rho_0+3p_0)-\omega^2\mathrm{e}^{-2\nu_0}\right]H_1(0)\right\}, \qquad (16)\\
Q_1 =& \frac{2}{l(l+1)}\left[\frac{1}{\gamma_0p_0}\mathrm{e}^{-\nu_0}X(0)+\frac{3}{2}K(0)+\frac{4\pi}{3}(l+1)\rho_0W(0)\right]. \qquad (17)
\end{aligned}$$

The evaluation of the second-order terms $Y_{,rr}(0)$ involves an expansion of the TOV equations as a power series also

$$p(r) = p_0+\frac{1}{2}p_2r^2+\frac{1}{4}p_4r^4+O(r^6), \qquad (18)$$

$$\rho(r) = \rho_0+\frac{1}{2}\rho_2r^2+O(r^4), \qquad (19)$$

$$\nu(r) = \nu_0+\frac{1}{2}\nu_2r^2+\frac{1}{4}\nu_4r^4+O(r^6). \qquad (20)$$

Using the TOV equations, one can obtain

$$\begin{aligned}
p_2 =& -\frac{4\pi}{3}(\rho_0+p_0)(\rho_0+3p_0), \qquad (21)\\
\rho_2 =& \ p_2(\rho_0+p_0)/(\gamma_0p_0), \qquad (22)\\
\nu_2 =& \ \frac{4\pi}{3}(\rho_0+3p_0), \qquad (23)\\
p_4 =& -\frac{2\pi}{5}(\rho_0+p_0)(\rho_2+5p_2)\\
&-\frac{2\pi}{3}(\rho_2+p_2)(\rho_0+3p_0)\\
&-\frac{32\pi^2}{9}\rho_0(\rho_0+p_0)(\rho_0+3p_0), \qquad (24)\\
\nu_4 =& \ \frac{2\pi}{5}(\rho_2+5p_2)+\frac{32\pi^2}{9}\rho_0(\rho_0+3p_0). \qquad (25)
\end{aligned}$$

At the surface of the star $r = R$, we demand that both the pressure and the Lagrangian change of the pressure vanish. This implies that some terms in Eq. (9c) are singular at $r = R$, requiring a special handling. If a finite differencing scheme is used for the solving of the differential equations, the outermost grid point within the star must be placed at $r = R_{\mathrm{G}}$ for some $R_{\mathrm{G}} < R$. We need to translate the boundary condition $X(R) = 0$ to the point $r = R_{\mathrm{G}}$.

For a star described by the EOS

$$p = p(\rho), \tag{26}$$

the adiabatic index γ is given by

$$\gamma = \frac{\rho + p}{p}\frac{\mathrm{d}p}{\mathrm{d}\rho}. \tag{27}$$

If the EOS is taken to be polytropic, i.e.,

$$p = \kappa\rho^{1+1/N}, \tag{28}$$

where κ and N are constants, near the surface of the star R

$$p = a(R-r)^{N+1}, \tag{29}$$

$$\rho = b(R-r)^{N}. \tag{30}$$

The constants a, b, R, and N are determined by requiring that p, ρ, and $\mathrm{d}p/\mathrm{d}r$, be continuous functions at R_{G}. Integrating the TOV equations from R to R_{G} assuming ρ is small but positive (note that $\rho < 0$ at $r = R_{\mathrm{G}}$ could happen due to numerical accuracy caused by a choice of R_{G} close to R), we obtain

$$R = R_{\mathrm{G}} - (N+1)\frac{p(R_{\mathrm{G}})}{p_{,r}(R_{\mathrm{G}})}. \tag{31}$$

It follows that $X(r)$ varies as

$$X(r) = c(R-r)^{N+1}. \tag{32}$$

We may choose freely the boundary values of the functions H_1, W, and K at R_{G}. Substituting these values into equation (9d), we can evaluate $X_{,r}(R_{\mathrm{G}})$. Using equation (32), we obtain

$$X(R_{\mathrm{G}}) = \frac{R_{\mathrm{G}} - R}{N+1}X_{,r}(R_{\mathrm{G}}). \tag{33}$$

Equation (33) serves as the boundary condition of $X(r)$ at $r = R_{\mathrm{G}}$.

2.3. The perturbed system for $r > R$

In general, outside the star the perturbed metric describes a combination of outgoing and incoming gravitational waves. We are interested particularly in the case of purely outgoing waves, representing the QNMs of the stellar model.

Outside of the star, the perturbation functions which describe the motion of the fluid vanish, i.e. $W = 0$, $X = 0$. The perturbation equations reduce to a second-order system, namely the Zerilli equation[55–57]

$$\frac{\mathrm{d}^2 Z}{\mathrm{d}r^{*2}} + \left[\omega^2 - V(r^*)\right] Z = 0, \tag{34}$$

where the effective potential $V(r^*)$ is given by

$$V(r^*) = \frac{2(1-2M/r)}{r^3(nr+3M)^2}[n^2(n+1)r^3 + 3n^2Mr^2 + 9nM^2r + 9M^3]. \tag{35}$$

Here r^* is the so-called "tortoise" coordinate, related to r by

$$r^* = r + 2M\log\left(\frac{r}{2M} - 1\right), \tag{36}$$

and $n = (l-1)(l+2)/2$. In terms of the metric perturbation functions $H_0(r)$ and $K(r)$, the Zerilli function $Z(r^*)$ and its first-order derivative are

$$Z(r^*) = \frac{k(r)K(r) - a(r)H_0(r) - b(r)K(r)}{k(r)g(r) - h(r)}, \tag{37}$$

$$\frac{\mathrm{d}Z(r^*)}{\mathrm{d}r^*} = \frac{h(r)K(r) - a(r)g(r)H_0(r) - b(r)g(r)K(r)}{h(r) - k(r)g(r)}. \tag{38}$$

Here $a(r)$, $b(r)$, $g(r)$, $h(r)$, and $k(r)$ are respectively

$$a(r) = -(nr+3M)/\left[\omega^2r^2 - (n+1)M/r\right], \tag{39}$$

$$b(r) = \frac{\left[nr(r-2M) - \omega^2r^4 + M(r-3M)\right]}{(r-2M)\left[\omega^2r^2 - (n+1)M/r\right]}, \tag{40}$$

$$g(r) = \frac{\left[n(n+1)r^2 + 3nMr + 6M^2\right]}{r^2(nr+3M)}, \tag{41}$$

$$h(r) = \frac{\left[-nr^2 + 3nMr + 3M^2\right]}{(r-2M)(nr+3M)}, \tag{42}$$

$$k(r) = -r^2/(r-2M). \tag{43}$$

The Zerilli equation has two linearly independent solutions $Z_+(r^*)$ and $Z_-(r^*)$ representing respectively incoming and outgoing waves. The general solution is given by their linear combination

$$Z(r^*) = A(\omega)Z_-(r^*) + B(\omega)Z_+(r^*). \tag{44}$$

At large radius, Z_+ and Z_- can be expanded as

$$Z_-(r^*) = \mathrm{e}^{-\mathrm{i}\,\omega r^*}\sum_{j=0}^{\infty}\beta_j r^{-j}, \tag{45}$$

$$Z_+(r^*) = \mathrm{e}^{\mathrm{i}\,\omega r^*}\sum_{j=0}^{\infty}\bar{\beta}_j r^{-j}, \tag{46}$$

where $\bar{\beta}_j$ is the complex conjugate of β_j. Substituting Eq. (45) (keeping terms to $j = 2$) into the Zerilli equation (34), we obtain

$$\beta_1 = -\,\mathrm{i}(n+1)\omega^{-1}\beta_0, \tag{47}$$

$$\beta_2 = -\omega^2\left[\frac{1}{2}n(n+1) - \frac{3}{2}\,\mathrm{i}\,M\omega\left(1+\frac{2}{n}\right)\right]\beta_0. \tag{48}$$

We note that in the expression for β_2 we have corrected a factor of 2 error in the second term of Eq. (A40) of LD.[9]

3. Implementation of the formulation

In this section, we describe in detail the numerical implementation of the formulation given in Section 2 above for the determination of the QNM frequencies for the case of $l = 2$.

The main part in the numerical implementation is the solving of the differential system (9) inside the star and Eq. (34) outside the star. We use the IMSL Gear[58] predictor–corrector integration routine. The spatial integration is separated into small steps (e.g., 10^4 steps for the radius of the star) with integration error (TOL) controlled to a level of 10^{-12}. As will be discussed below, another important ingredient is the solving of linear system of equations with real or complex coefficients, for which the LINPACK[59] routine is used.

In the sample problem given in this section, we use a stellar model with a polytropic EOS. We give explicit results in various intermediate steps of the calculation, so that future researchers have numbers to compare to in applying the formulation.

3.1. The equilibrium model

We take as a model a TOV star with the polytropic EOS, $p = \kappa\rho^{\Gamma}$. Here ρ is the total density of energy, and p is the pressure. A direct integration of the TOV Eqs. (2)–(5) above with the central density of $\rho_0 = 0.00486$ and for the EOS of $\kappa = 46$ and $\Gamma = 2$ gives an equilibrium model with a total mass $M = 1.269223984$, in units of $G = c = 1$ and the solar mass $M_\odot = 1$ (the same units are used throughout the paper). We take the radius of the star to be at $R = 6.00524$, where $\rho(R) = 4.982227883 \times 10^{-9}$ and $p(R) = 1.141839355 \times 10^{-15}$, i.e., a radius where ρ and p are effectively zero.

3.2. Treatment at $r = 0$

Because the system of differential equations is singular at $r = 0$, we need to start the numerical integration from a point $r_0 > 0$. We expand the functions of perturbation at $r = 0$ in the form of Eq. (11). At $r = 0$, there are two degrees of freedom for the perturbation. We follow LD[9] and choose $W(0) = 1$ and $K(0) = \pm(\rho_0 + p_0)$. The three remaining boundary values $H_0(0)$, $H_1(0)$, and $X(0)$ are determined by equations (12)–(14). For our system of interest it is straightforward to confirm that, in the range of r_0 of order 0.01, one needs to take the expansion only to the second order (e.g., for our model star of $\rho_0 = 0.00486$ and a frequency of interest, $\omega = 0.0888$ (see below)). The second order term is of order 10^{-8} of the zero order term.

We examine the dependence of the final result on the choice of r_0. In Fig. 1, we plot the real part of the lowest $l = 2$ QNM frequency against the choice of r_0 for our sample problem with all other numerical parameters fixed. We see that the frequency is unchanged up to the tenth digit in its real part and ninth digit in its imaginary part for r_0 in the range 0.0006 to 0.01. This indicates that r_0 in this range is a suitable choice (for this sample problem). For r_0 smaller than 0.0006, the integration becomes unstable and is sensitive to the choice of r_0 (with the numerical integration scheme we use) due to the $1/r$ singularity in the differential system. On the other hand, for r_0 larger than 0.01, the error from the expansion (11) is large. As shown in Fig. 1, the error grows as the fourth power of r_0 (c.f. Eq. (11)). A fitted line of power r^4 is given as the box-dashed line starting at 0.025 for comparison. We see the two lines overlap to high accuracy. The dependence of the imaginary part of the QNM frequency on r_0 is exactly the same as the real part and is not repeated here. Henceforth in the rest of the sample calculation we choose $r_0 = 0.01$ which is approximately $0.0016652R$ in terms of the radius R of the equilibrium star.

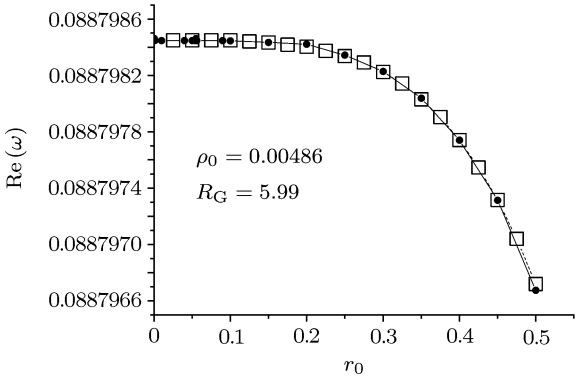


Fig. 1. The effect of r_0 on the real part of the lowest QNM frequency of the sample system (dot–solid line). r_0 is the starting point of integration. End point of the integration is taken to be $R_{\rm G} = 5.99$.

3.3. Treatment of boundary conditions at the surface of star $r = R$

At the surface of the star the boundary condition demands that the pressure vanish (i.e. $p(R) = 0$), and the Lagrangian change in the pressure vanish. This implies $X(R) = 0$ where X is defined by Eq. (10). The perturbation system containing $1/p$ terms is singular at R due to the boundary condition.

We denote the last point of integration inside the star by $R_{\rm G}$. Obviously $R_{\rm G}$ cannot be taken too close to R due to integration problem, nor too far away from R for accuracy consideration, in a situation similar to the choice of r_0. A convenient way to see how to choose $R_{\rm G}$ is to make use of Eq. (31). Given any $R_{\rm G}$, one can calculate an R value based on Eq. (31), which can be compared with the value obtained in the equilibrium profile.

In our sample problem, we have the equilibrium radius $R = 6.00524$ (where $\rho(R) = 4.982227883 \times 10^{-9}$). If we take $R_{\rm G} = 5.99$, equation (31) gives an R value of $R = 6.00519$, which is off by 0.0008% and is accurate enough.

To examine the dependence of the final result on the choice of $R_{\rm G}$, we plot the real and imaginary parts of the QNM frequency versus different choices of $R_{\rm G}$ in Fig. 2. (To put the real and imaginary parts on the same scale, we have multiplied the imaginary part by 1.96×10^3.) We see that the real and imaginary parts exhibit basically the same behaviour, namely in a range of $R_{\rm G} < R$, they stay constant to a high precision until $R_{\rm G}$ is too close to R. For the choice of integration parameters used, figure 2 shows that $R_{\rm G}$ should be less than 5.994 for a reliable integration. We set $R_{\rm G}$ to $5.99 \approx 0.99746R$ for the rest of this sample calculation. Equation (31) gives an R value within 10^{-7} of the correct value.

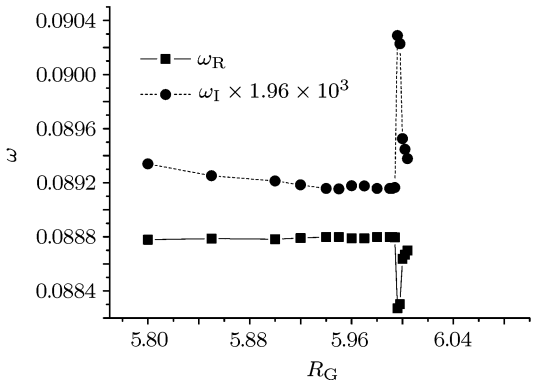


Fig. 2. The effect of $R_{\rm G}$ on the frequency of QNM with $\rho_0 = 0.00486$. The symbol $\omega_{\rm R}$ denotes the real part of the frequency, and $\omega_{\rm I}$ is the imaginary part. $R_{\rm G}$ is the outermost grid point inside the star.

3.4. Matching at $r = r_{\rm c}$

To satisfy the boundary conditions both at r_0 and $R_{\rm G}$, we integrate Eqs. (9) from r_0 forward and from $R_{\rm G}$ backward to a point $r = r_{\rm c}$ somewhere inside the star, say, $r_{\rm c} = R/2$, and match the two sets of solutions.

For the backward integration from $R_{\rm G}$, with the four differential equations (Eqs. (9)) and with the value of $X(R_{\rm G})$ specified, there are $4 - 1 = 3$ linearly independent solutions to work with, which we denote $\boldsymbol{Y}_1$, $\boldsymbol{Y}_2$, and $\boldsymbol{Y}_3$. For example, at $R_{\rm G}$, $\boldsymbol{Y}_1$ can be a solution having $H_1 = 0.004$, $K = 0.01$, and $W = 1.0$, $\boldsymbol{Y}_2$ can be a solution having $H_1 = 0.001$, $K = 0.1$, and $W = 0.01$, while $\boldsymbol{Y}_3$ can be $H_1 = 0.06$, $K = 0.04$, and $W = 0.1$. Starting with these values and the value of $X(R_{\rm G})$, we integrate Eqs. (9) from $R_{\rm G}$ to $r_{\rm c}$ to determine $\boldsymbol{Y}_1$, $\boldsymbol{Y}_2$, and $\boldsymbol{Y}_3$.

On the other hand, we integrate Eqs. (9) forward from r_0 with the conditions (13), (14), which leave $4 - 2 = 2$ degrees of freedom. For these two degrees of freedom we follow LD/DL to take ($W(0) = 1$, $K(0) = (\rho_0 + p_0)$) as one choice and ($W(0) = 1$, $K(0) = -(\rho_0 + p_0)$) as the other choice. As these two choices are given at $r = 0$ we first have to translate them to r_0 using Eq. (11) with the coefficients given by Eqs. (12)–(25). For our sample problem, e.g., for $\omega = 0.0888$, this yields at r_0 the following two sets of values ($H_1(r_0) = 5.378179109170230 \times 10^{-2}$, $K(r_0) = 5.946498826857080 \times 10^{-3}$, $W(r_0) = 1.00000423560485$, $X(r_0) = 6.541124451203853 \times 10^{-5}$) and ($H_1(r_0) = 4.585310846964769 \times 10^{-2}$, $K(r_0) = -5.946489270502415 \times 10^{-3}$, $W(r_0) = 1.00000345922029$, $X(r_0) = 4.746606257676690 \times 10^{-5}$). (We have given many digits of results not for their accuracy, but for the comparison of future work following the treatment.) Integrating with these values from r_0 forward yields two linearly independent solutions from r_0 to $r_{\rm c}$, denoted as $\boldsymbol{Y}_4$ and $\boldsymbol{Y}_5$.

The matching of the solutions at $r_{\rm c}$ amounts to finding a linear combination of $\boldsymbol{Y}_4$ and $\boldsymbol{Y}_5$ that is the same as a linear combination of $\boldsymbol{Y}_1$, $\boldsymbol{Y}_2$, and $\boldsymbol{Y}_3$; such a solution would then satisfy the boundary conditions both at $r = 0$ and $r = R$. This leads to

$$\begin{aligned} &\alpha_1 \boldsymbol{Y}_1(R/2) + \alpha_2 \boldsymbol{Y}_2(R/2) + \alpha_3 \boldsymbol{Y}_3(R/2) \\ &= \alpha_4 \boldsymbol{Y}_4(R/2) + \alpha_5 \boldsymbol{Y}_5(R/2). \end{aligned} \tag{49}$$

Among the five α_i, one of them is an arbitrary constant controlling the size of the linear perturbation. We take $\alpha_5 = 1$. With $\boldsymbol{Y}$ representing H_1, K, W, and X, we have four equations for the four unknown

α_i. The resulting α_i give a physical solution in the domain $0 \le r \le R$.

Two further points of this matching process are to be discussed in order. While in principle, we can specify whatever values we like for the five free degrees of freedom (two at $r = 0$ and three at $r = R$), however a random choice often yields a set of ($\boldsymbol{Y}_1$, $\boldsymbol{Y}_2$, $\boldsymbol{Y}_3$) having some components with magnitudes very different from those of ($\boldsymbol{Y}_4$, $\boldsymbol{Y}_5$) at $r_{\rm c}$. The solving of the linear equations at $r_{\rm c}$ yields a set of α_i containing some large values. The accuracy of the numerical calculation in solving the linear Eqs. (49) would be comprised. In our sample calculation we keep the values of α_i in the range 10^{-3} to 10^3, which can be achieved without much difficulties in tuning the starting values of ($\boldsymbol{Y}_1$, $\boldsymbol{Y}_2$, $\boldsymbol{Y}_3$).

For our sample calculation, e.g., for $\omega = 0.0888$, the choice of ($H_1 = 0.004$, $K = 0.01$, $W = 1.0$; $H_1 = 0.001$, $K = 0.1$, $W = 0.01$; $H_1 = 0.06$, $K = 0.04$, $W = 0.1$) at $R_{\rm G}$ leads the set of α (0.814116868300915, -0.110831458946552, $3.200981407777719 \times 10^{-3}$, -0.649853317007167, 1), when the matching point is chosen to be $r_{\rm c} = 3.0$.

Another point to note is the choice of $r_{\rm c}$. The final result should be independent of the value of $r_{\rm c}$. For our sample problem, we have checked that within the range $r_c = 0.8$ to 5.5, the QNM frequency would remain basically the same: The real part of the frequency would not change with respect to different choices of $r_{\rm c}$ up to at least the ninth digit, while the imaginary part sixth digit in all calculations perform (we require higher accuracy in some calculations).

3.5. Determining the boundary condition for the external problem

Next we go on to integrate the Zerilli equation in the vacuum region outside the star starting from R. To determine the boundary value to start with at R, we need to find H_0 and K at R in order to determine Z and its first derivative according to Eqs. (37) and (38).

From the set of α_i determined, and the set of $\boldsymbol{Y}_1$, $\boldsymbol{Y}_2$, $\boldsymbol{Y}_3$ chosen at $R_{\rm G}$, we can find the values of $(W(R_{\rm G}), K(R_{\rm G}), H_1(R_{\rm G}), X(R_{\rm G}))$ that belong to the correct perturbation solution that satisfies all boundary conditions for a given ω.

As an example, for our sample calculation, for $\omega = 0.0888$, with the α_i given above, we have ($H_1(R_{\rm G}) = 3.337694898723957 \times 10^{-3}$, $K(R_{\rm G}) = -2.813937955335342 \times 10^{-3}$, $W(R_{\rm G}) = 0.813328651851147$, $X(R_{\rm G}) = 1.361863068268735 \times 10^{-10}$).

However, this is just at $R_{\rm G}$ and we have to extend the solution to R. A direct integration of Eqs. (9) would not work, with its singular terms at R, otherwise we would not have to set an $R_{\rm G} < R$ in the first place. Instead, we substitute all appearances of p, ρ and X in Eqs. (9) by the expressions (29), (30) and (32) respectively and simplify; this gets rids of all singular behaviour of the system and allows the integration from $R_{\rm G}$ to R.

The value of $X(R)$ so obtained provides an accuracy check of the rather complicated calculation up to this point. In all of our calculations, we check and make sure that $X(R)/X(r_0)$ is always less than 10^{-8} in all of our calculations (and better in cases necessary).

For our sample calculation, with $\omega = 0.0888$, we have ($H_1(R) = 3.285293660922767 \times 10^{-3}$, $K(R) = -2.776240696612714 \times 10^{-3}$, $W(R) = 0.816552243049889$, $X(R) = 7.773267834522427 \times 10^{-14}$), and $Z(R) = -1.065253316165201 \times 10^{-2}$, and $\mathrm{d}z/\mathrm{d}r(R) = 3.982246562852239 \times 10^{-3}$. Again, we are reporting these numbers with many digits not for the accuracy, but for convenience of comparison of future researchers repeating the treatment.

3.6. Integrating the Zerilli equation from R to infinity

For $r > R$, the perturbation system reduces to the Zerilli equation (34). It is straightforward to integrate it to a large radius, which we take to typically $r = 50\omega^{-1}$. A large enough radius far out in the wave zone is necessary for a meaningful discussion of incoming and outgoing waves, and the use of the asymptotic forms of Z_- (45) and Z_+ (46) takes only the first 3 terms in the expansions, as discussed below. We have checked convergence with respect to the size of the computational domain up to $r = 500\omega^{-1}$.

3.7. Determining the QNM frequencies

For real ω, the solutions of the Zerilli equation represent standing waves; the incoming and outgoing amplitudes are complex conjugates of each other

$$A(\omega) = B^*(\omega). \tag{50}$$

From the numerical values of Z and $\mathrm{d}z/\mathrm{d}r$ at $r = 50\omega^{-1}$, equation (44) gives a $B(\omega)$, the incoming wave amplitude which is a complex number, for each real ω.

Next, we assume that $B(\omega)$ is an analytic function of ω and proceed to determine this function as a power series

$$B(\omega) = \gamma_0 + \gamma_1\omega + \gamma_2\omega^2, \tag{51}$$

where γ_0, γ_1 and γ_2 are complex constants and we omit higher order terms. In principle, carrying out the above calculation with three different real ω would suffice to determine γ_0, γ_1 and γ_2. The QNM frequency corresponding to the absence of incoming radiation would then be determined (finally!) as the root (the one with a positive imaginary part) of

$$B(\omega) = \gamma_0 + \gamma_1\omega + \gamma_2\omega^2 = 0. \tag{52}$$

In practice, instead of accepting the resulting ω immediately as the final result, we note that the accuracy of this procedure depends on the three real ω chosen to be close enough to the QNM ω in the complex plane. Once the first trial QNM ω is obtained, we use the value of its real part, and choose a new set of three real ω closer to this value and repeat the calculation. This process is repeated until the real part value of the QNM ω converges to the eighth digit. For this sample problem, the imaginary part would also converge to at least the fifth digit at the same time. (For the cases of large Q, higher accuracy would be required.)

Through the above steps we obtained for our sample problem the lowest $l = 2$ QNM frequency to be $\omega = 8.8798460 \times 10^{-2} + \mathrm{i} \times 4.5488 \times 10^{-5}$. In comparison, Balbinski *et al.*[13] obtained for the same case $\omega = 8.8807 \times 10^{-2} + \mathrm{i} \times 4.5474 \times 10^{-5}$. The discrepancy is small for this case of $Q \sim 10^3$.

4. Determination of accuracy and improvement

There are three types of error in going from the analytic formulation to the final numerical value of the frequency: (i) computer machine precision, (ii) finite differencing error in numerical integration and error in linear solver algorithm, and (iii) errors introduced by the approximations in the treatment, in particular, 1) the expansion at r_0, 2) the expansion at r_{G}, and 3) the expansion of out-going wave amplitude $A(\omega)$ at infinity (the outer boundary of computation) in terms of the frequency.

With the speed and memory of modern computers, the error source (i), i.e. computer machine precision, is not a concern. One can always use quadruple (or higher) precision if needed, although in our present case double precision is enough for our purpose in view of the other types of inaccuracy.

Modern numerical algorithms for numerical integration and linear solvers make (ii) not a concern. Predictor–corrector algorithm as the one used in our implementation guarantees the overall error of integration to be smaller than a specified value. Typically we take it to be 10^{-12}, which is enough in view of the error type (iii).

Error type (iii): We find this type to be the most difficult sources of error in our error study. In Section 3, we provided analyses of the errors introduced in the expansion at r_0 and the expansion at R_{G}. An analysis of the error associated with the expansion of the out-going wave amplitude $A(\omega)$ is more complicated. When one goes into using higher order terms in the expansion, more points of the real frequency inputs would have to be used. The best range of the real frequencies used as inputs cannot be determined a priori and this in turn depends on the magnitude of the imaginary part of the frequency to be determined. Instead of going into a detailed study of this error source, we develop a separate treatment to measure directly the overall accuracy of the QNM frequency obtained.

The requirements on the QNM frequency are 1) it is a complex eigen-frequency corresponding to an eigen-function satisfying the boundary conditions at $r = 0$ and $r = R$, and 2) it produces a $B(\omega)/A(\omega) = 0$ at infinity. For a frequency satisfying 1), the error can be measured directly by the value of $S(\omega) = |B(\omega)/A(\omega)|$ it produces, where $|\ \ |$ denotes taking the absolute value. As QNMs with long decay time, the focus of this paper, are sharp resonances, $S(\omega)$ is an accurate measure of the accuracy.

To determine $S(\omega)$ for a complex ω we repeat the treatment described in Section 3. That is, for a given complex ω, we repeat the treatments at $r = 0$ and $r = R$ with all functions now regarded as complex and we solved for a set of complex α_i at $r = r_{\mathrm{c}}$. This gives us a solution satisfying all boundary conditions, with errors under control as discussed above. Next we integrate this solution to the outer boundary of the computational domain and evaluate $S(\omega)$. The outer boundary is typically taken to be $r_{\mathrm{b}} = 50\omega^{-1}$ in our implementation. The error introduced by a finite r_{b} can be determined by a convergence test with respect to increasing r_{b} . We found that for all ω's studied in this paper, $S(\omega)$ is accurate up to 10^{-4} for $r_{\mathrm{b}} = 50\omega^{-1}$. With this understanding, $S(\omega)$ at

$r_{\rm b} = 50\omega^{-1}$ is a measure of the accuracy of the complex QNM frequency found.

Next we turn to the central issue of our paper, namely the determination of QNM frequencies of long living modes, i.e., modes with large $Q = \omega_{\rm R}/(2\omega_{\rm I})$. In Fig. 3, we plot $S(\omega)$ against $\log_{10}(Q)$. The solid boxes denote the QNMs obtained as outlined in Section 3 of this paper. For Q of order 10^5 or smaller, $S(\omega)$ is smaller than 10^{-3}, indicating highly accurate results. However we see that as Q increases to above 10^7, despite our best effort in controlling the sources of error as discussed in Section 3 above, $S(\omega)$ shoots up to that of order 1.

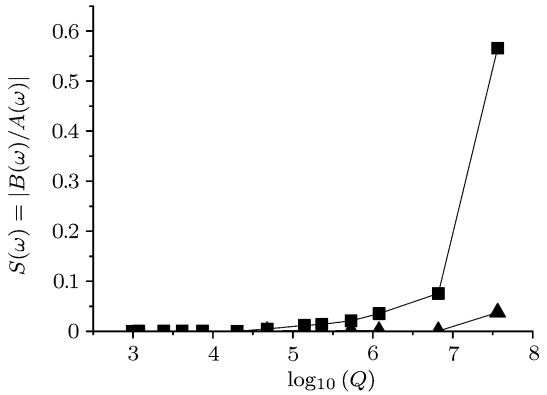


Fig. 3. $S(\omega)$ plotted against $\log_{10}(Q)$. The solid boxes represent values obtained using the treatment given in Section 3. The triangles are those obtained by refining the solid boxes with the 2D search minimizing $S(\omega)$.

This brings us to the point of the refinement of the frequencies obtained. With $S(\omega)$ being a sensitive indicator of the accuracy, it is straightforward to implement a two-dimensional numerical search for the real and imaginary parts of the frequency to minimize $S(\omega)$, starting with the frequencies obtained through the treatment outlined in Section 3 above. We implement such a search and obtain the triangles for each of the solid box in Fig. 3. Through this last step, we determined the QNM frequency up to $Q \sim 10^8$ with an imaginary part having 3 digits of precision.

In view of this, one might be tempted to start off with a complex frequency treatment using just the complex analogy of the steps (a) to (h) in Section 3 and do without step (g). However, we note that the difficulty of doing the search directly is that $S(\omega)$ is a very sensitive function of ω only in a narrow range of ω near the actual QNM frequency. For a frequency which is not close to the actual QNM frequency either in the real or the imaginary part, $S(\omega)$ is of order 1. In order to start a search, one needs to have a rather accurate first guess. The step (g) can be regarded as providing such a first guess (or one may begin with a known QNM of a close enough neighbouring stellar configuration).

5. Conclusions

In this paper we gave a treatment based on the DL/LD formulation[9,10] that is capable of determining long living QNMs of (non-rotating) relativistic stars, treating the fully coupled set of the spacetime and fluid equations without simplifying assumptions. We show that the QNMs with an imaginary part of the frequency eight orders of magnitudes less than the real part can be determined accurately.

The treatment can be used for the investigation of the p mode QNM series, pushing beyond the first few p modes. The determination of the p mode series has been argued in Ref. [24] to have implication on the life time of gravitational wave sources and stellar stability. The study of the QNMs with less compact stars could also be carried out using this treatment.

The paper contains a detailed presentation of the various numerical choices and the intermediate results with an aim to facilitate researchers to make use of the treatment.

Acknowledgment

We thank Steven Detweiler, P. T. Leung, and Hui-Min Zhang for their communications and suggestions.

References

[1] http://www.ligo.caltech.edu
[2] http://lisa.nasa.gov
[3] http://www.virgo.infn.it
[4] Thorne K S and Campolattaro A 1967 *Astrophys. J.* **149** 591
[5] Price R and Thorne K S 1969 *Astrophys. J.* **155** 163
[6] Thorne K S 1969a *Astrophys. J.* **158** 1
[7] Thorne K S 1969b *Astrophys. J.* **158** 997
[8] Campolattaro A and Thorne K S 1970 *Astrophys. J.* **159** 847
[9] Lindblom L and Detweiler S L 1983 *Astrophys. J. Suppl.* **53** 73
[10] Detweiler S L and Lindblom L 1985 *Astrophys. J.* **292** 12

[11] Chandrasekhar S and Ferrari V 1991 *Proc. R. Soc. Lond.* A **432** 247
[12] Ferrari V 1992 *Phil. Trans. R. Soc. Lond.* A **340** 423
[13] Balbinski E, Detweiler S and Schutz B F 1985 *Mon. Not. R. Astron. Soc.* **213** 553
[14] Ipser J R and Thorne K S 1973 *Astrophys. J.* **181** 181
[15] Detweiler S L 1975 *Astrophys. J.* **201** 440
[16] Lindblom L and Splinter R S 1989 *Astrophys. J.* **345** 925
[17] Chandrasekhar S and Ferrari V 1991 *Proc. R. Soc. Lond.* A **434** 449
[18] Price R H and Ipser J R 1991 *Phys. Rev.* D **44** 307
[19] Chandrasekhar S and Ferrari V 1992 *Proc. R. Soc. Lond.* A **437** 133
[20] Kokkotas K D and Schutz B F 1992 *Mon. Not. R. Astron. Soc.* **255** 119
[21] Leins M, Noller H P and Soffel M H 1993 *Phys. Rev.* D **48** 3467
[22] Kokkotas K D 1994 *Mon. Not. R. Astron. Soc.* **268** 1015
[23] Andersson N and Kokkotas K D 1996 *Phys. Rev. Lett.* **77** 4134
[24] Andersson N, Kokkotas K D and Schutz B F 1995 *Mon. Not. R. Astron. Soc.* **274** 1039
[25] Andersson N, Kokkotas K D and Schutz B F 1996 *Mon. Not. R. Astron. Soc.* **280** 1230
[26] Andersson N and Kokkotas K D 1998 *Mon. Not. R. Astron. Soc.* **299** 1059
[27] Allen G, Andersson N, Kokkotas K D and Schutz B F 1998 *Phys. Rev.* D **58** 124012
[28] Kokkotas K D and Stergioulas N 1999 *Astron. Astrophys.* **341** 110
[29] Andersson N and Kokkotas K D 1999 *Mon. Not. R. Astron. Soc.* **320** 307
[30] Benhar O, Berti E and Ferrari V 1999 *Mon. Not. R. Astron. Soc.* **310** 797
[31] Yip C W, Chu M C and Leung P T 1999 *Astrophys. J.* **513** 849
[32] Kokkotas K D and Ruoff J 2001 *Astron. Astrophys.* **366** 565
[33] Ruoff J and Kokkotas K D 2001 *Mon. Not. R. Astron. Soc.* **328** 678
[34] Kojima Y and Sakata K 2002 *Prog. Theor. Phys.* **108** 801
[35] Sotani H and Harada T 2003 *Phys. Rev.* D **68** 024019
[36] Sotani H, Khori K and Harada T 2004 *Phys. Rev.* D **69** 084008
[37] Benhar O, Ferrari V and Gualtieri L 2004 *Phys. Rev.* D **70** 124015
[38] Kokkotas K D 2005 *Nucl. Phys. Proc. Suppl.* **138** 433
[39] Samuelsson L, Andersson N and Maniopoulos A 2007 *Class. Quantum Grav.* **24** 4147
[40] Finn L S 1987 *Mon. Not. R. Astron. Soc.* **227** 265
[41] McDermott P N 1990 *Mon. Not. R. Astron. Soc.* **245** 508
[42] Strohmayer T E 1993 *Astrophys. J.* **417** 273
[43] Miniutti G, Pons J A, Berti E, Gualtieri L and Ferrari V 2003 *Mon. Not. R. Astron. Soc.* **338** 389
[44] Ferrari V, Miniutti G and Pons J A 2003 *Mon. Not. R. Astron. Soc.* **342** 629
[45] Ferrari V, Gualtieri L, Pons J A and Stavridis A 2004 *Mon. Not. R. Astron. Soc.* **350** 763
[46] Ferrari V, Gualtieri L and Pons J A 2007 *Class. Quantum Grav.* **24** 5093
[47] Ferrari V, Gualtieri L and Marassi S 2007 *Phys. Rev.* D **76** 104033
[48] Gaertig E and Kokkotas K D 2008 *Phys. Rev.* D **78** 064063
[49] Gaertig E and Kokkotas K D 2009 *Phys. Rev.* D **80** 064026
[50] Lau H K, Leung P T and Lin L M 2010 *Astrophys. J.* **714** 1234
[51] Stergioulas N 1996 http://ads.bao.ac.cn/abs/1996PhDT.....4S
[52] Ott C D, Burrows A, Dessart L and Livne E 2006 *Phys. Rev. Lett.* **96** 201102
[53] Fu W J, Wei H Q and Liu Y X 2008 *Phys. Rev. Lett.* **101** 181102
[54] Cowling T G 1942 *Mon. Not. R. Astron. Soc.* **101** 367
[55] Zerilli F J 1970 *Phys. Rev. Lett.* **24** 737
[56] Fackerell E D 1971 *Astrophys. J.* **166** 197
[57] Chandrasekhar S and Detweiler S 1975 *Proc. R. Soc. Lond.* A **344** 441
[58] http://www.vni.com/products/imsl/
[59] http://www.netlib.org/linpack/